Available online at www.sciencedirect.com
SCIENCE DIRECT®
International Journal of Thermal Sciences 43 (2004) 509–517
International Journal of Thermal Sciences
www.elsevier.com/locate/ijts

A simulation code for batch heat treatments

Luca A. Tagliafico *, Maurizio Senarega

DITEC, Energy and Environmental Conditioning Department, University of Genoa, Via all'Opera Pia 15/a, 16145 Genoa, Italy

Received 21 January 2003; accepted 25 September 2003

Abstract

The paper describes a numerical model that uses a finite-difference technique to simulate 2D-thermal transients of solid and hollow cylinders in convective and radiant cavities with participating media and time-dependent wall cavity temperatures. The model takes into account all the thermo-physical property variations with temperature of both gases and materials under treatment. These last (usually named "load") are subject to strong nonlinear thermal boundary conditions and must undergo given thermodynamic transitions.

The proposed model is validated with respect to the solutions obtained by other calculation techniques for some simplified problems. Simple thermal transients (cooling) are considered for constant-property cylinders in a convective environment, the analytical solution being taken as a reference. Simplified radiation cases are also examined and the solutions yielded by the model are compared with those given by a finite element commercial code (ANSYS®).

Stability and accuracy characteristics of the calculation algorithm are identified as a function of operating conditions and discretization criteria (discretized Biot and Fourier numbers).

Keywords: Batch furnaces; Heat treatments; Numerical heat transfer

1. Introduction

Heat treatment consists of a sequence of heating and cooling stages under controlled conditions in order to achieve given temperature cycles inside the materials being treated. The aim of the heat treatment is to develop the required thermodynamic, morphological or chemical-physical transitions in the materials. The procedure finds application in numerous fields, from the food industry (e.g., baking ovens, frozen food production) to the production of electronic components (silicon component heat treatment) and several industrial applications, the most important being in iron and steel production. There are many different heat treatment processes. A common type uses intermittent-operation furnaces, which are usually named batch furnaces, as a certain quantity of material (load) is loaded inside, to be taken out of the furnace when the treatment is completed.

The two main technological requirements of this process are temperature uniformity for all the pieces inside the furnace and strict control of the exposure time to fixed temperature levels. Actually, the control system cannot directly measure the internal temperature of the pieces being treated. Usually one or two temperature values are measured on furnace walls and inside the gaseous atmosphere in the furnace. The availability of a tool able to calculate the thermal fields inside both "load" and furnace walls, when the heating profile of internal gases and surface walls are given, is fundamental for control and design purposes.

For example, during the design stage, furnace dimensions and layout can be optimised, as can the internal geometrical arrangement of the load. During operation, scheduling of proper temperature levels for the furnace and residence time for the load can be optimised, thus reducing the cost of installation and operation as well as production cycle times. Furthermore, product quality and uniformity can be improved, while at the same time decreasing energy consumption and the environmental impact of the process.

There are basically three different ways of obtaining information on design and operating conditions for high-temperature industrial furnaces:

(i) measurements on operating furnaces,
(ii) physical modelling using small-scale laboratory models, and
(iii) mathematical simulation of the system.

* Corresponding author.
E-mail addresses: tgl@ditec.unige.it (L.A. Tagliafico), senarega@ditec.unige.it (M. Senarega).

1290-0729/$ – see front matter
doi:10.1016/j.ijthermalsci.2003.09.005

Nomenclature

A	surface	m^2
Bi	Biot number	
b_n	eigenvalue	
c	specific heat	$J{\cdot}kg^{-1}{\cdot}K^{-1}$
D	diameter	m
F	radiative view factor	
Fo	Fourier number	
h	heat transfer coefficient	$W{\cdot}m^{-2}{\cdot}K^{-1}$
H	height	m
i, j	finite difference spatial coordinates	
J_0, J_1	Bessel functions	
k	thermal conductivity	$W{\cdot}m^{-1}{\cdot}K^{-1}$
K	thermal conductance	$W{\cdot}K^{-1}$
K_n	coefficients	
L	length	m
n	finite difference time step	
N	number of discretized intervals	
q'''	rate of heat generation per unit volume	$W{\cdot}m^{-3}$
q	heat transfer rate	W
r	radial coordinate	m
R	radius	m
T	temperature	K
x, y	Cartesian coordinate	

Greek symbols

Δ	finite difference	
δ	thickness	m
ε	thermal emissivity	
η	weight	
θ	angle (coordinate)	rad
Θ	dimensionless temperature	
ρ	density	$kg{\cdot}m^{-3}$
σ	Stefan Boltzmann constant, $= 5.67 \times 10^{-8}$	$W{\cdot}m^{-2}{\cdot}K^{-4}$
τ	time	s

Subscripts

C	convective
c	on the cylinder axis (center)
E	on external surface
ext	external
gas	of (to) the gas
i	generic numeral
int	internal
j	generic numeral
k	conductive
p	of the furnace walls
R	radiative
walls	to the furnace walls
θ	at (along) the θ coordinate
θ_1	of the cylinder surface #1
θ_2	of the cylinder surface #2
0	initial ($\tau = 0$)

Superscripts

I	of the first region
II	of the second region
III	of the third region
IV	of the fourth region
n	at the time step n

The cost of the first method and the modelling difficulties of the second make them impractical. In particular, the second method does not provide some of the most relevant information about the system, namely the radiation heat transfer from high-temperature combustion products, since this cannot be obtained from any "low-temperature" scaled model.

The third method is therefore the most promising evaluation tool, in that it is able to assess given operating conditions and rate new design alternatives at relatively low cost. However, before any mathematical model can be confidently used to simulate the system, it must be validated by independent data (i.e., experimental measurements [1–3] and theoretical results [1]).

1.1. Review of literature

Several calculation models are available in the literature to tackle the general problem of transient convection–radiation heat transfer in furnaces for heat treatment in several fields of application. These studies mainly concern the handling of the complicated load–gas–furnace radiative interactions, and of the related apparent or mean emissivity/absorptivity properties of the participating media.

The most simplified models neglect temperature gradients inside the load, focusing on the problem of load distribution inside the furnace to achieve global temperature uniformity during the thermal transient. For instance, [4] studies vacuum furnaces heated by several radiant tube burners and enclosed within thermal insulation walls. Materials to be heated are placed in the central region of the furnace. To solve the combined problem of conductive (inside the furnace walls) and radiant (between heating surfaces and load) transient heat transfer, a three-dimensional model has been developed with the Monte Carlo method of calculating radiative heat exchange. In this model each part of the load is assumed to be at a uniform internal temperature, equal to the temperature of the furnace volume where it is located. Some comparisons between numerical results and experimental measurements show a good fit. The approach, which is successful in this case with a relatively small furnace volume (around 1 m^3), cannot give any indication of internal temperatures of the pieces under treatment.

Precise thermal control of multi-zone batch furnaces has become increasingly important in the semiconductor industry to prevent defects from being generated during device fabrication. This type of batch thermal reactor consists of three key elements: a stack of wafers, some electrical resistive heaters and a fused silica process tube. The simulation model developed in [5] has two significant thermal features: the radial temperature distribution on wafers follows a universal parabolic profile and the wafer stack gives rise to a strong cavity effect, which produces thermal radiation. The aim of that work was to characterise the dependence of wafer temperature nonuniformity on processing conditions, including the ramp rate and wafer spacing. For this geometry (wafer diameter $D = 200$ mm, wafer thickness $\delta = 0.725$ mm and spacing between wafers from 5 mm to 25 mm), the transient thermal problem can be solved much more simply by introducing a time-dependent parabolic-type temperature distribution inside the cylinder, over a wide range of temperatures, operating conditions and system regulation strategies.

When the furnace size and the load mass become large (e.g., single cylinder 1 m in diameter and furnace length around 30 m) a full analysis of the time–temperature profiles inside each component of the "load" and of the furnace walls is needed in order to accurately predict the temperature distribution over time.

A simulation model for natural gas, direct-fired batch and continuous furnaces has been developed in [6]. Radiative heat transfer to the load is calculated by considering the thermal interactions among the load (consisting of a single rectangular slab in a pre-fixed position), combustion products and refractory walls, using Hottel's zone method [7]. The radiative heat flux was calculated assuming mean emissivity and absorptivity, and using the Monte Carlo method coupled to the sum-of-four-grey-gases model. The authors report a series of parametric results for both types of furnace examined, concluding that the simulation model defined is an efficient tool for predicting system behaviour and for making preliminary choices in order to optimise the design and basic working conditions. The effects of the load surface and refractory wall emissivities on load surface and combustion gas temperature and on the total heat flux to the load along the furnace are analysed in detail. The results obtained also show the effect of load and refractory surface emissivities on furnace efficiency.

Temperature uniformity is of particular relevance for steel bars that are discharged from reheating furnaces for subsequent rolling. Indeed, nonuniformity of the stock discharge temperature may cause unacceptable variations in thickness during rolling, and thus influence the quality of the final product. In order to optimise the heating process modes and times/slab velocity, a three-dimensional finite-element mathematical model has been developed [1], which provides deep knowledge of the nonstationary temperature field in rectangular blocks of steel. The model is validated with respect to an analytical solution, a numerical solution obtained from a commercial code [8] and full-scale experimental data.

Further studies are available for cases in which the load is not homogeneous and the internal temperature distribution is of particular relevance. In [9] rolled steel coils in an HPH (High Performance Hydrogen) furnace have been considered as a periodically multi-layer material in the radial direction, and a new formula for determining the radial equivalent thermal conductivity has been proposed. Several experimental measurements of internal temperatures of rolled coils have been taken in order to validate the numerical model. The annealing temperature curves calculated by using the radial equivalent thermal conductivity show good agreement with experimental data.

1.2. The present model

This paper focuses on the problem of transient temperature profiles inside loads made up of several cylinders (solid or hollow) during heat treatment in batch furnaces. The geometry is 2-D and all the thermo-physical properties are assumed to be temperature-dependent. Nonhomogeneous loads (rolls, packed beds, and so on) can be studied by properly modelling the equivalent thermal conductivity of the porous material [9,10].

The model developed within this research activity is based on a finite-difference approach and shows some significant advantages in calculation when compared with the codes described above:

- the definition of load geometry and the arrangement of the load inside the furnace are more general and more flexible;
- the internal temperature can be calculated exactly even when thermo-physical properties vary considerably with temperature; consequently, processes involving thermodynamic phase transitions and nonhomogeneous media can also be simulated;
- effective computation, as already in [1], of radiant effects and participating gases inside the furnace;
- by means of a simple space/time transformation, it can also simulate "continuous" processes, in which a uniformly distributed load proceeds at constant speed through the furnace.
- as simulation time is shorter, complex optimisation algorithms can be exploited.

The paper reports preliminary checks of the model, in which the numerical results are compared with other theoretical solutions obtained for the two following cases:

(i) analytical solution for the particularly easy case of 1-D thermal transient with purely convective boundary conditions

(ii) finite-element solution (ANSYS®) for the 2-D case with only radiant thermal exchange between furnace walls and load, and with nonparticipating gas.

Finally, an actual industrial application has been simulated, by comparing program results with ANSYS® data in a particular complete batch treatment process. Analysis of calculation performance shows that the program can simulate a 197-hours transient process in just 11s calculation time, which is less than one fortieth of the time taken by the ANSYS® program. This performance is achievable provided that a proper compromise among stability, precision and number of time steps is found. Further improvements may be achieved by introducing into the calculation program a dynamic time-step variation during the simulation.

2. Problem formulation

The study of the heat treatment of rolls, cylinders and similar objects was carried out with reference to the general pattern of load geometry shown in Fig. 1. The rectangular cross section of the furnace is filled with cylindrical bars located (or forwarded) longitudinally. The load pattern is ensured by appropriate refractory supports, which are not shown in the figure.

In high-temperature furnaces, radiation is the main heat transfer mechanism. As known, radiation generally depends on the geometry, relative orientation, temperature and radiant properties of the surfaces and finally on the characteristics of the gaseous medium in-between (semi-transparent media affecting considerably the intensity of thermal radiation which passes through).

Under these conditions, the fluid dynamics of gases inside the furnace and the related distribution of convective heat transfer coefficients are second-order accuracy terms of the global thermal problem and can be approximately assigned as given operating data. The atmosphere inside the furnace consists of flue gases. The present study refers mainly to heat treatments where the temperature gradients inside the material are by far the most crucial issue of the process and the composition and temperature of the flue gases can be assumed known and approximately uniform.

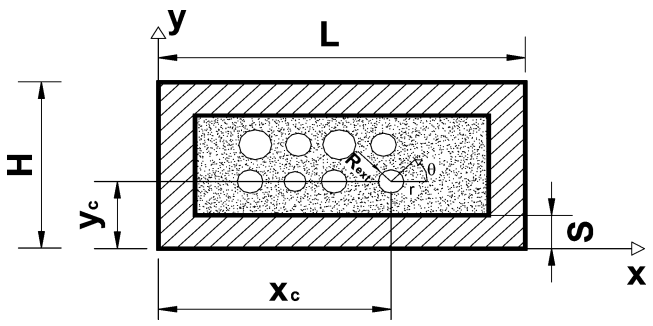

Fig. 1. Sketch of a simplified furnace section with cylindrical load.

The system model is transient in time and 2-D in geometry. The furnace is a rectangular cavity (width × height $L \times H$) containing the load (cylinders with axis located along coordinate x_c, y_c) and the gases. The problem of 2-D conduction inside each cylinder with radius R_i and longitudinal axis located at coordinates x_i and y_i, is solved with reference to a local system of polar coordinates (r, θ), while the global model has a Cartesian reference system (x, y).

The radiative heat transfer in the presence of a participating gas should be evaluated by the global balance of radiation intensity in each space direction, considering emission, absorption and scattering phenomena [11]. Nevertheless, the solution of the entire problem is extremely complex and requires long calculation times. Therefore, in engineering applications, simplified approaches are used. In this work, scattering effects have been neglected. This approach makes the net radiation method, which is traditionally used to study radiation in the presence of transparent media, also applicable to problems involving a participating gas [11,12]. The application of this method requires that the radiation properties of the gas be defined, as in the treatment of solid surfaces in cavities. It can be used only for uniform thermodynamic conditions of the gas itself, i.e., without significant gradients of pressure, temperature, composition and concentration.

2.1. Mathematical model

Referring to a generic cylinder with external radius R_e, the conduction problem inside the load can be properly treated by a system of polar coordinates centred on each cylinder axis. The general equation of conduction in a system of polar coordinates (r, θ) becomes:

$$\frac{1}{r}\frac{\partial}{\partial r}\left(rk\frac{\partial T}{\partial r}\right)+\frac{1}{r}\frac{\partial}{\partial \theta}\left(\frac{k}{r}\frac{\partial T}{\partial \theta}\right)+q'''=\rho c\frac{\partial T}{\partial \tau} \tag{1}$$

where q''' [W·m^{-3}] is the rate of heat generation per unit volume, k [W·m^{-1}·K^{-1}] the thermal conductivity, ρ [kg·m^{-3}] the density and c [J·kg^{-1}·K^{-1}] the specific heat.

2.1.1. Discretized equations

To obtain discretized equations, Eq. (1) is multiplied by r ($\neq 0$) and integrated with respect to r and θ on the control volume shown in Fig. 2: as $r \cdot \mathrm{d}r \cdot \mathrm{d}\theta$ is the value of the volume of an axial element of unitary depth, this is the same as calculating a volume integral [13].

With reference to Fig. 2, the conduction equation is discretized in polar coordinates. Furthermore, assuming that only thermodynamic transitions of the second-order type take place in the material, the internal heat generation due to phase transition can be simulated by means of suitable specific heat variations with temperature. Thus, the following equation is obtained for each node (i, j):

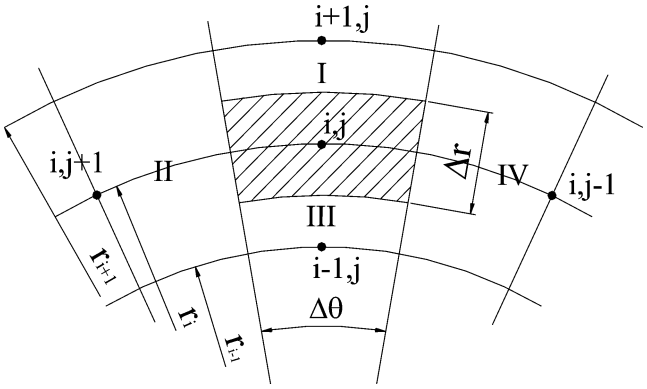

Fig. 2. Control volume in polar coordinates.

$$\begin{aligned}
&\left[\frac{k^{\mathrm{I}}}{r_{i+1}-r_i}\Delta\theta\left(\frac{r_i+r_{i+1}}{2}\right)(T_{i+1,j}-T_{i,j})\right.\\
&\quad+\frac{k^{\mathrm{II}}}{r_i\Delta\theta}\left(\frac{r_{i+1}+r_{i-1}}{2}\right)(T_{i,j+1}-T_{i,j})\\
&\quad+\frac{k^{\mathrm{III}}}{r_i-r_{i-1}}\Delta\theta\left(\frac{r_{i-1}+r_i}{2}\right)(T_{i-1,j}-T_{i,j})\\
&\quad\left.+\frac{k^{\mathrm{IV}}}{r_i\Delta\theta}\left(\frac{r_{i+1}+r_{i-1}}{2}\right)(T_{i,j-1}-T_{i,j})\right]\\
&=\rho c\frac{\pi}{N_\theta}\left(\frac{r_{i+1}^2-r_{i-1}^2}{2}\right)\left(\frac{T_{i,j}^{n+1}-T_{i,j}^{n}}{\Delta\tau}\right) \qquad (2)
\end{aligned}$$

where N_θ is the number of circumferential nodes and $\Delta\tau$ is the time step of integration.

All thermal conductivities k are calculated at the spatial average between the temperatures of adjacent nodes, while density and specific heat in the node (i, j) are calculated at the temperature averaged between time instants n and $(n+1)$. According to whether the terms on the left side of the equation are referred to a time step n or $n+1$, the explicit or implicit formulation of the discretized conduction equation is obtained. When a weight $0<\eta<1$ is defined, the explicit form of the Eq. (2) is multiplied by $(1-\eta)$ and the implicit one by η, the sum of the obtained equations gives the weighted average of the explicit and implicit formulations, as used in this model (Eq. (3)). Considering $\eta=0.5$, i.e., calculating the arithmetic mean between two formulations, the Crank–Nicholson method is obtained [13].

Final discretized equation (internal points):

$$\begin{aligned}
&\frac{k^{\mathrm{I}}}{r_{i+1}-r_i}\Delta\theta\left(\frac{r_i+r_{i+1}}{2}\right)\left[(1-\eta)T_{i+1,j}^{n}+\eta T_{i+1,j}^{n+1}\right]\\
&\quad+\frac{k^{\mathrm{II}}}{r_i\Delta\theta}\left(\frac{r_{i+1}+r_{i-1}}{2}\right)\left[(1-\eta)T_{i,j+1}^{n}+\eta T_{i,j+1}^{n+1}\right]\\
&\quad+\frac{k^{\mathrm{III}}}{r_i-r_{i-1}}\Delta\theta\left(\frac{r_{i-1}+r_i}{2}\right)\left[(1-\eta)T_{i-1,j}^{n}+\eta T_{i-1,j}^{n+1}\right]\\
&\quad+\frac{k^{\mathrm{IV}}}{r_i\Delta\theta}\left(\frac{r_{i+1}+r_{i-1}}{2}\right)\left[(1-\eta)T_{i,j-1}^{n}+\eta T_{i,j-1}^{n+1}\right]\\
&\quad+\left[-\frac{k^{\mathrm{I}}}{r_{i+1}-r_i}\Delta\theta\left(\frac{r_i+r_{i+1}}{2}\right)\right.\\
&\quad-\frac{k^{\mathrm{II}}}{r_i\Delta\theta}\left(\frac{r_{i+1}+r_{i-1}}{2}\right)-\frac{k^{\mathrm{III}}}{r_i-r_{i-1}}\Delta\theta\left(\frac{r_{i-1}+r_i}{2}\right)\\
&\quad\left.-\frac{k^{\mathrm{IV}}}{r_i\Delta\theta}\left(\frac{r_{i+1}+r_{i-1}}{2}\right)\right]\left[(1-\eta)T_{i,j}^{n}+\eta T_{i+1,j}^{n+1}\right]\\
&=\rho c\frac{\pi}{N_\theta\Delta\tau}\left(\frac{r_{i+1}^2-r_{i-1}^2}{2}\right)\left(T_{i,j}^{n+1}-T_{i,j}^{n}\right) \qquad (3)
\end{aligned}$$

2.1.2. Boundary conditions

Proper boundary conditions have to be associated to the conduction equation (3) by calculating, in each surface node, the external heat transfer rate q_E exchanged between the load surface and the outside. The external heat flow rate q_E can be separated into convective (q_C), conductive (q_k), and radiative (q_R) heat transfer rates. Convection takes place with the gas inside the furnace, and is evaluated by means of a surface conductance h_C, which, in general, can vary in time and space (in any case according to a given, known law) around the cylinder. Conduction is present if one or more points of the surface of the cylinder are in contact with other solids (i.e., with another cylinder, with furnace walls or supports) and can be expressed by means of an equivalent contact resistance. The radiant contribution can be sub-divided into one term due to the furnace walls and another one due to the participating gas. Since the actual aim of the heat treatment furnace is to ensure good temperature uniformity among the various load elements, radiant heat exchange between different cylinders have been neglected. Given the discretized external surface area of the cylinder $A_\theta = R_{\mathrm{ext}}\Delta\theta$, the following set of boundary conditions is obtained:

$$q_E = q_C + q_k + q_R \qquad (4a)$$

$$q_{C\theta} = h_{C\theta}A_\theta(T_{\mathrm{gas}} - T_\theta) \qquad (4b)$$

$$q_k = K(T_{\theta_1} - T_{\theta_2}) \qquad (4c)$$

$$q_R = (q_R)_{\mathrm{walls}} + (q_R)_{\mathrm{gas}} \qquad (4d)$$

$$(q_R)_{\mathrm{walls}} = \sum_{j=1}^{4}\frac{\sigma(T_{p_j}^4 - T_\theta^4)}{\frac{1-\varepsilon_\theta}{\varepsilon_\theta A_\theta}+\frac{1}{A_\theta F_{\theta j}(1-\varepsilon_g)}+\frac{1-\varepsilon_j}{\varepsilon_j A_j}} \qquad (4e)$$

$$(q_R)_{\mathrm{gas}} = \frac{\sigma(T_g^4 - T_\theta^4)}{\frac{1-\varepsilon_\theta}{\varepsilon_\theta A_\theta}+\frac{1}{A_\theta F_{\theta g}\varepsilon_g}} \qquad (4f)$$

where, θ_1 and θ_2 are the coordinates of the contact point between two adjacent cylinders.

For the purpose of the evaluations carried out in this paper, (q_k) and $(q_R)_{\mathrm{gas}}$ are not needed in the calculations, in spite of their being the main issue of a specific study, which, for the sake of brevity, is not described here. In Eq. (4d), A_j [m^2] represents the area of each surface of the furnace wall.

In radiation heat transfer, the view factors F, i.e., the energy fraction emitted by a surface and incident onto another, must be calculated. Analytical values, tabulations or diagrams of view factors are available for a limited number of fairly simple geometries. In actual structures, the geometric shape of surfaces is complicated and rays

from surfaces A_θ to surface A_j may be partially intercepted (shadow phenomenon). No analytical expression is therefore available for $F_{\theta j}$, which means that approximate numerical methods have to be used.

The "Crossed-Strings Method" [14] and the Monte Carlo method [15] have been adopted in the present model, without discretizing each of the four flat furnace walls, for reasons of simplicity. As known, the first method can be employed only for 2-D geometries, in long cavities with constant cross-section, as in the case here considered.

2.1.3. Numerical solution

The numerical solution of the mathematical model solves the resulting strongly-nonlinear set of algebraic equations by means of an iterative solution based on the linear solver available in FORTRAN IMSL mathematic libraries [16]. Nonlinearities are due to the dependence of thermo-physical properties on temperature and to marked time variations in external heat flow rates (mainly due to the radiation term in boundary conditions). Furthermore, time-dependent boundary conditions are handled. During iterations, properties and heat transfer rates are calculated with reference to a temperature field corresponding to the algebraic mean between values (known) at instant n and values (unknown) at the following instant $(n+1)$. Convergence is checked by using the maximum percentage difference between temperature values of two successive iterations (usually a calculation step is assumed to have been completed when five significant digits are stabilised).

3. Numerical model validation

3.1. 1-D transient conduction in a long cylinder when physical properties and boundary conditions are both constant

Many analytical solutions are available in literature to determine the transient temperature field inside solids. In general, these solutions refer to solids with constant thermo-physical properties and simplified geometries and boundary conditions [17].

The transient temperature field inside a solid cylinder of infinite length, radius R, constant thermo-physical properties and initial temperature T_0, located in a convective environment at temperature T_∞, where the heat transfer rate is calculated by means of the constant radiative-convective coefficient α, can be obtained analytically. The exact solution depends on three nondimensional groups (r/R, $Bi = \alpha R/k$, $Fo = a\tau/R^2$) and is available in the form of a series of infinite terms [12]:

$$\Theta = \frac{T(r,\tau) - T_\infty}{T_0 - T_\infty} = \sum_{n=1}^{\infty} K_n J_0\left(b_n \frac{r}{R}\right) e^{-b_n^2 Fo} \tag{5}$$

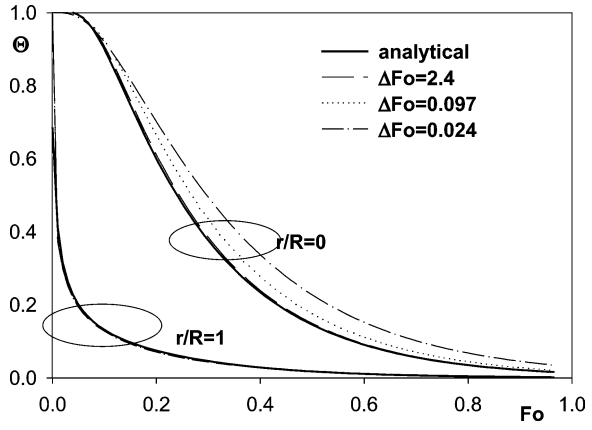

Fig. 3. Comparisons among the theoretical (analytical curves (Eq. (5))) and numerical results in a 1-D cooling process. $Bi = 10$, $\Delta\tau = 50$ s, variable number of radial nodes (5–10–50).

with the coefficients K_n expressed as:

$$K_n = \frac{2\,Bi}{(b_n^2 + Bi^2)\cdot J_0(b_n)} \tag{6}$$

where eigenvalues b_n are the roots of the equation:

$$b_n \cdot J_1(b_n) - Bi \cdot J_0(b_n) = 0 \tag{7}$$

where J_0 and J_1 are the Bessel functions.

The convergence of the series (5), when the Fourier number is small ($Fo < 0.05$), is possible only with a very large number of terms; this number increases as the Biot number increases [12]. In this paper 20 terms are used [18], and reliable values are obtained with $Bi = 10$ starting from $Fo > 0.04$.

Fig. 3 shows trends of nondimensioned temperatures on the external surface ($r/R = 1$) and cylinder axis ($r/R = 0$), for different discretized Fourier numbers ($\Delta Fo = a\Delta\tau/\Delta r^2$), as a function of nondimensional time (Fo). By comparing these trends to the theoretical solution based on Eq. (5), it can be observed that for a fixed time-step ($\Delta\tau = 50$ s), the accuracy of the numerical solution of the cylinder surface does not depend on mesh dimension Δr, while the accuracy of temperature results on the axis is strongly affected.

By contrast, for coarse meshes, the reduction of time-steps does not improve accuracy even if numerical instability effects are removed, as is well known from literature [13] (Fig. 4).

In general, comparison between theoretical results and results obtained from the calculation program shows that the model gives lower values than the series data on the cylinder surface, and higher values on the axis.

Finally, it is to be noted that Biot number values exceeding 10 correspond to very sharp thermal transients, with very high internal temperature gradients. This condition gives rise, as usual in finite difference numerical apporaches, to particular problems in terms of the expected stability and accuracy of the numerical solutions obtained.

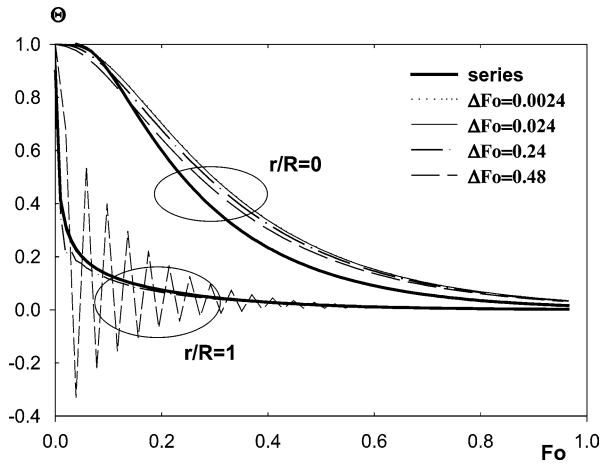

Fig. 4. Comparison of numerical over analytical results for $Bi = 10$, with different time steps: $\Delta\tau = 5$, 50, 500, 1000 s—5 radial nodes—threshold of stability $\Delta Fo \approx 0.48$.

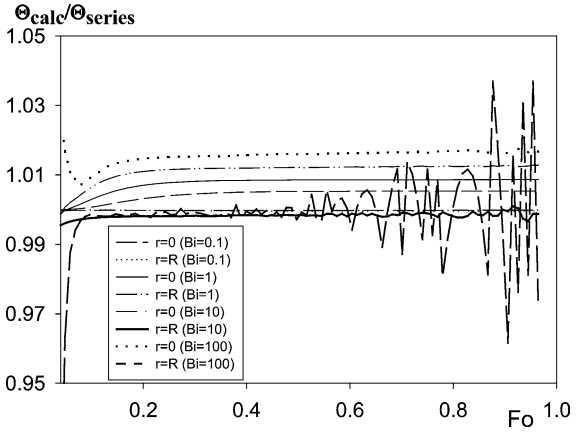

Fig. 5. Comparison of numerical over analytical results, with variable Biot number.

Fig. 5 shows the comparison, in terms of non-dimensional variables, between the model and theoretical (serial development with 20 terms) solutions for temperature profiles on the external surface and on the axis, with Biot number values 0.1, 1, 10 and 100. It can be observed that the maximum differences (on axis $r = 0$) increase as the Biot number increases, but are always lower than 2% even at $Bi = 100$. These differences are partially due to intrinsic limits in the series solution, which always gives values below the exact solution [12, Fig. 4.10], especially when $Fo < 1$. The oscillations evidenced in the figure for high Biot number values ($Bi = 10$, $Bi = 100$) are not wrong or unstable numerical calculations, but oscillations due to truncation errors in the calculation of the asymptotic solution ($\Theta \to 0$), which are quickly reached for lower Fo numbers when Bi is high.

Numerical stability of the calculation algorithm has been checked over a large range of Biot and discretized Fourier numbers, proving that the Crank–Nicholson method used in this case is stable up to maximum values $\Delta Fo = 2$ ($\Delta Fo < 2$). This limit value decreases as Bi increases (in Fig. 4, $\Delta Fo_{\lim} = 0.48$ with $Bi = 10$; in the case of Fig. 4 accuracy is compromised by the low number of nodes).

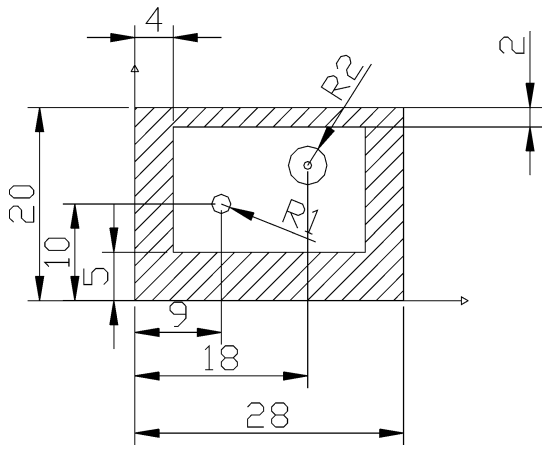

Fig. 6. Sketch of the modelled furnace (geometrical dimensions in meters).

Further tests, not reported here for sake of brevity, proved that, provided the already mentioned limits on Bi and ΔFo are respected, stability and accuracy characteristics of the calculation method are not significantly affected by non-linear boundary conditions (radiant exchanges) coupled to simultaneous phase transitions inside the material.

3.2. Radiant thermal exchanges of a cylinder in an isothermal rectangular cavity

The calculation criteria applied to view factors in the algorithm and the evaluation of radiant contributions to thermal heat transfer rate were first checked by assuming negligible convective contributions and studying the heating of two cylinders made of carbon steel (0.06% C) and subjected to a phase transition during the heat treatment inside a nonsymmetrical batch furnace. The geometrical system is sketched in Fig. 6.

The thermo-physical properties are strongly variable with temperature, furnace walls are assumed at a constant temperature—different for each side—and cylinder and wall radiant properties are constant and equal. This problem was also solved by means of a commercial code (ANSYS®, available at DITEC).

3.2.1. Description of the ANSYS® model

The system shown in Fig. 6 was modelled in ANSYS® by following the definition procedure of a "radiative matrix" [19]. The definition of this matrix, which represents the radiant heat transfer rate of a particular thermal superelement, allows the program to calculate the view factors for arbitrarily oriented surfaces. However, it does not allow the dependence of surface emissivity on temperature to be taken into account. Therefore, emissivity has been assumed to be constant and equal to 0.8, for both furnace walls and load (i.e., cylinders).

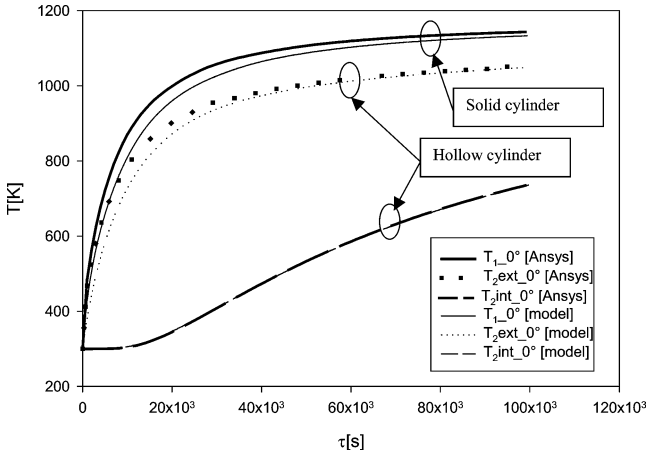

Fig. 7. Surface temperature of the two cylinders and internal temperature of the hollow one for $\theta = 0°$: comparison between the results of ANSYS® and the present model.

3.2.2. Comparisons between the results of the two calculation methods

Comparison of the time–temperature curves obtained for the heating process of a load consisting of a couple of cylinders (one hollow and one solid) initially at 300 K temperature is performed. The cylinders are located in a furnace with the four walls subjected to a step increase in temperature up to 1273 K, 1100 K, 1000 K, and 1100 K respectively (counter-clockwise starting from the bottom). The comparison reveals that the maximum difference in cylinder surface temperature between the two models is about 70 K (Fig. 7).

This difference is mainly due to the different integration criteria used to calculate the radiative heat transfer. Moreover, while in ANSYS the furnace walls are discretized, in our model they are not. Since the temperature is uniform and constant on each furnace wall, this simplification affects only the view factor calculations, and has a very slight influence. This comparison confirms the adequate capacity of the calculation model to simulate solid thermal transients under variable thermo-physical properties, even with strongly non-linear boundary conditions, such as in radiant environments.

4. Example of batch heat treatment

The model set-up has been applied to the calculation of an actual batch furnace process, to test calculation speed and the possibility of obtaining reliable results in short calculation times. This feature is a mandatory requirement if the calculation program is to be used in much more complicated optimisation algorithms for design and control purposes.

4.1. System description

The actual furnace with two possible cylinder arrangements is sketched in Fig. 8. For brevity only the two-cylinder

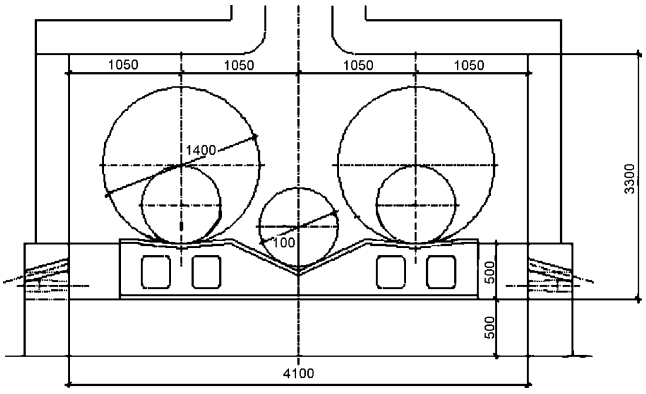

Fig. 8. Sketch of the cross-section of the heat treatment batch furnace (geometrical dimensions in millimetres).

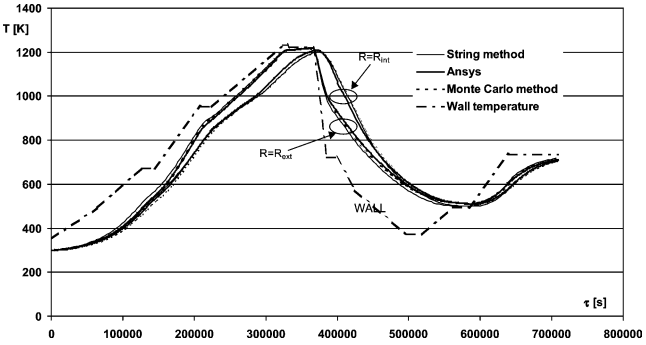

Fig. 9. Temperature variations of furnace walls (given data, dashed line) and cylinder temperatures obtained with different calculation methods (R_{int} = on the cylinder axis, R_{ext} = on the external surface of the cylinder).

configuration results are reported here. Qualitatively similar results can be obtained for the three-cylinder arrangement. In this first trial simulation, the thermal interactions between the cylinder and its support have been neglected and uniform convective heat transfer coefficients are assumed all around the cylinder. To make solutions comparable to ANSYS® data, uniform and constant thermal emissivities are assumed, without participating gas.

The thermal treatment cycle takes the form of a set of wall temperature ramps imposed with a given timing, as shown in Fig. 9 (dashed line).

The aim of the calculation is to give the temperature history inside the cylinders, to compare the data obtained by means of different codes, and, if necessary, to compare them to actual, measured temperatures inside the furnace and inside the load material.

4.2. Simulation results

The results obtained are reported in Fig. 9, in which the cylinder temperature response is reported for a given temperature history of the heating furnace walls.

The temperature curves can be referred to either of the two cylinders, owing to the symmetry of geometry and boundary conditions along a vertical plane. The numerical problem has been solved for the entire furnace with both

cylinders, proving that the numerical solutions comply exactly with this simmetry condition.

The comparison between the ANSYS® model and the present numerical model is reported in Fig. 9 for two different calculation methods of the view factors: the string method and the Monte Carlo method respectively. All the results show quite good agreement, thus confirming the reliability of the calculation method described. Moreover the execution time is quite short: in the order of 10 s simulation time for a 200 hours treatment process (on an 800 MHz CPU personal computer with NT2000 operating system and Compaq 6.0 Fortran compiler).

5. Conclusions

A calculation model has been described for the 2-D simulation of thermal transients of solid and hollow cylinders inside convective and radiant cavities, with participating media and cavity walls with given variable temperature. The model takes into account the dependence of all thermo-physical properties on temperature, both for any gases present and solid materials, including the effect of second-order thermodynamic transitions.

The results of the numerical model have been compared with solutions obtained with other theoretical methods (analytical and finite elements) for two simplified problems. The first is related to thermal transients (cooling) of homogeneous cylinders at constant physical properties in a constant, uniform convective environment. The second treats radiant heating of steel cylinders inside a rectangular furnace with given wall temperature hystories.

Comparisons confirmed the good simulation features of the model set-up, even at fairly long time-integration intervals and with a strong nonlinear equation system, owing to both thermo-physical property variations with temperature and to radiative heat transfer boundary conditions.

In particular, it has been pointed out that:

- even with very high Biot numbers ($Bi = 100$), the difference between theoretical and calculated non-dimensional temperature curves does not exceed 2%;
- the threshold of numerical stability, in terms of the discretized Fourier number ($\Delta Fo = a\Delta\tau/\Delta r^2$) is correlated to Bi values with $\Delta Fo < 2$ for Bi in the range 0.1–1, in the order of $\Delta Fo < 0.5$ for $Bi = 10$, down to $\Delta Fo < 0.1$ when $Bi = 100$;
- the crossed-strings method is accurate enough for relatively simple geometries, but the use of the Monte Carlo method is mandatory when complicated geometries are to be studied;
- calculation speed is quite satisfactory, making the numerical program suitable for use in much more complicated optimisation algorithms for design and control purposes.

Acknowledgements

This study has been developed in the framework of technical-scientific co-operation between the Energy and Environmental Conditioning Department, University of Genoa and the Company Techint S.p.A.

Special thanks to Eng. Massimiliano Fantuzzi for his help in technical discussions and granting databanks concerning the thermo-physical properties of steel.

References

[1] D. Lindholm, B. Leden, A finite element method for solution of the three-dimensional time-dependent heat-conduction equation with application for heating of steels in reheating furnaces, Numer. Heat Transfer, Part A 35 (1999) 155–172.
[2] B. Leden, A. Rensgard, M. Korteniemi, Analysis of hot charging process for slabs by advanced simulation program Steeltemp® at Outokumpu Polarit's Hot Strip Mill in Tornio, Finland, Rev. Metallurgie CIT April (1994) 541–548.
[3] B. Leden, D. Lindholm, E. Nitteberg, The use of Steeltemp® Software in heating control, Rev. Metallurgie CIT Mars (1999) 367–380.
[4] A. Mochida, K. Kudo, Y. Mizutani, M. Hattori, Y. Nakamura, Transient heat transfer analysis in vacuum furnaces heated by radiant tube burners, Energy Convers. Manag. 38 (10–13) (1997) 1169–1176.
[5] Yong-Hui Fan, Taiqing Qui, Transient heat transfer in batch thermal reactors for silicon wafer processing, Internat. J. Heat Mass Transfer 41 (11) (1998) 1549–1557.
[6] R. Viskanta, K.S. Chapman, S. Ramadhyani, Mathematical modeling of heat transfer in high-temperature industrial furnaces, in: Proceedings of the International Conference on Advanced Computational Methods in Heat Transfer, 1990.
[7] H.C. Hottel, A.F. Sarofim, Radiative Heat Transfer, McGraw-Hill, New York, 1967.
[8] B. Leden, STEELTEMP®, A program for temperature analysis in steel plants, Scand. J. Metall. 15 (1986) 215–223.
[9] X. Zhang, Y. Zuo, W. Wu, Analytical and experimental study on radial equivalent thermal conductivity for steel coil heat transfer in HPH furnace, in: XII International Heat Transfer Conference, Grenoble, France, August 2002.
[10] G. Buonanno, F.A. Dell'Isola, G. Giovinco, Conducibilità termica equivalente di impaccamenti di sfere in aria: Indagine sperimentale, in: LVII ATI National Conference, Pisa, Italy, Settembre, 2002.
[11] R. Siegel, J.R. Howell, Thermal Radiation Heat Transfer, McGraw-Hill, New York, 1972.
[12] A. Bejan, Heat Transfer, Wiley, New York, 1993.
[13] M.N. Őzişik, Finite Difference Methods in Heat Transfer, CRC Press, Boca Raton, FL, 1994.
[14] F. Kreith, The CRC Handbook of Thermal Eng., Chapter 3, CRC Press, Boca Raton, FL, 2000.
[15] J.R. Howell, The Monte Carlo method in radiative heat transfer, J. Heat Transfer 120 (1998) 547–560.
[16] A.A. Vari, IMSL—Fortran Subroutines for Mathematical Applications, vols. 1 and 2, Visual Numerics, 1997.
[17] H.S. Carslaw, J.C. Jaeger, Conduction of Heat in Solids, Oxford University Press, Oxford, 1959.
[18] M. Senarega, L.A. Tagliafico; Sviluppo e verifica di un codice di calcolo per la simulazione di trattamenti termici in forni batch, in: XX UIT National Heat Transfer Conference, Maratea, Italy, June 2002.
[19] Manuale ANSYS®, Heat transfer training manual for release 5.7, 2001.